ISSN 1028-334X, Doklady Earth Sciences, 2016, Vol. 469, Part 1, pp. 705–709. © Pleiades Publishing, Ltd., 2016.
Original Russian Text © V.B. Lapshin, A.V. Patonin, A.V. Ponomarev, M.G. Potanina, V.B. Smirnov, S.M. Stroganova, 2016, published in Doklady Akademii Nauk, 2016, Vol. 469, No. 1, pp. 97–101.

GEOPHYSICS

Initiation of Acoustic Emission in Fluid-Saturated Sandstone Samples

V. B. Lapshin[a], A. V. Patonin[b], A. V. Ponomarev[c], M. G. Potanina[d], V. B. Smirnov[d], and S. M. Stroganova[c]

Presented by Academician A.O. Gliko May 13, 2015

Received May 25, 2015

Abstract—A rock behavior experiment with uniaxial compression revealed the effect of acoustic activity in loaded fluid-saturated Berea sandstone samples in response to an electric current. It is established that it is substantially intensified in periods of the current impact and decreases after its cut-off. The current impact also results in a growth of radial deformation indicating an increase in the sample volume. The effect of acoustic activation increases in response to increased heat emitted by the electric current during its flow through the sample, which allows the discovered effect to be explained by initiation of its destruction due to thermal expansion of the fluid in rock interstices and fissures.

DOI: 10.1134/S1028334X16070047

In relatively rare works dedicated to acoustic emission (AE) and its behavior in loaded rocks under the impact of an electric current, it was assumed that the electric field superimposed on deformed rock samples stimulates development of microfractures, which may result in the increased acoustic emission [1–3].

In some such experiments, monocrystals, minerals, and rocks were used [4, 5]. The results of these experiments indicate that the observable effects depend on many factors, such as the mineral composition, humidity of the test medium, parameters and conditions of the impact, and others and are determined by various mechanisms. For example, the mechanism of thermal AE stimulation [6] and the thermally stimulated mechanism of elastic wave damping in sandstones and granites under the impact of temperatures up to 600°C [7, 8] were discussed.

Investigations in this field of knowledge may be of importance for solving problems related to consequences induced by a strong electromagnetic impact on the real geological medium, assessment of seismotectonic deformations, stimulation of mechanical vibrations at deep levels, and others [9–11].

We investigated the AE parameters and their behavior under galvanic and noncontact electric impact on sandstone samples. The essential difference between our investigations and previous studies consists in the use of press equipment with a servo controller, which made it possible to conduct experiments under the influence of different controlled deformations during all the loading stages and application of methods and algorithms of the analysis applied in seismological practice, which increases substantially the reliability of interpretations of the available data.

The experiments were conducted on a servo controlled INOVA press and, partly, the RTR-4500 (GCTS) complexes. The complexes include sets of modules, which offered the opportunity to register synchronously the axial pressure, axial and radial deformations, P wave velocities along 16 propagation paths, wave shapes of individual acoustic events by 16 sensors mounted on the surface of test samples, the value of the acoustic emission flow from sensors built into press punches, and the surface temperature of samples [12]. The experimental data are gathered into a single database, which contains raw data and the results of their processing (catalogs and bulletins of acoustic events, tomographic sections of distributions

[a] *Fedorov Institute of Applied Geophysics, Russian Academy of Sciences, ul. Rostokinskaya 9, Moscow, 107258 Russia*
[b] *Borok Geophysical Observatory, Schmidt Institute of Physics of the Earth, Russian Academy of Sciences, Borok, Yaroslavl region, 152742 Russia.*
[c] *Schmidt Institute of Physics of the Earth, Russian Academy of Sciences, ul. Bolshaya Gruzinskaya 10, Moscow, 123995 Russia*
[d] *Physics Department, Moscow State University, Moscow, 119991 Moscow*
e-mail: potanina@physics.msu.ru

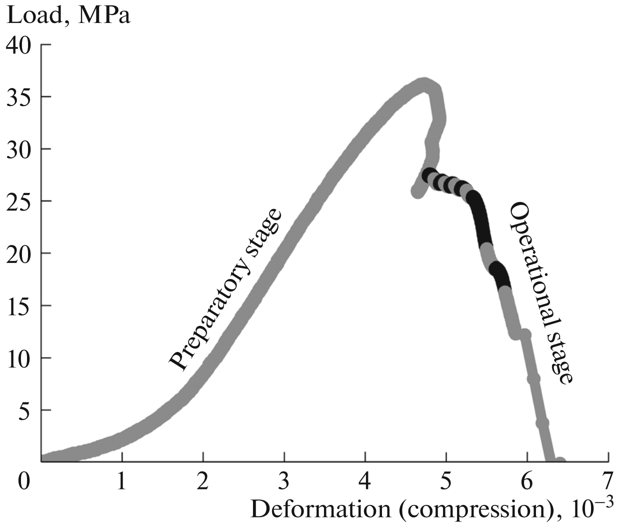

Fig. 1. An example of the loading curve. The dark color designates intervals of the electric current impact on the sample.

of P wave velocities in the sample body, projections of hypocenters of acoustic emission events for specified time intervals). The sources of direct and alternating current were used as generators of the electric field.

Cylindrical samples of Berea sandstone 30 mm in diameter and 60 mm high were subjected to the uniaxial load with a specified strain-control regime. At the preparatory stage, loading was carried out with a velocity of 2×10^{-6} 1/s; the stage terminated at the transition to the overcritical load, i.e., corresponding to the descending branch of the subsidence curve. It was followed by the second, operational stage, when loading was carried out with a substantially lower deformation velocity $(1–2) \times 10^{-7}$ 1/s or in the regime of constant deformation (Figs. 2, 3).

At the operational stage, the end faces of the sample were subjected to the impact of the difference of electric potentials in the interval of 60 to 1500 V. Electrodes for obtaining the difference of potentials were located between the press punches and the end faces of the sample and isolated from punches by glass fiber laminate spacers. The difference in the potential was provided during the specified time interval (usually 100, 300, 600 s) interrupted by similarly long pauses in the electric impact. During the experiment, the difference in the potential at electrodes and the current strength in the sample was controlled for estimating the electric power dispersed in the sample (the effect of polarization at the contact of electrodes with the sample was omitted from consideration).

The samples were saturated with a NaCl water solution (usually, 0.6N). The solution was added prior to the experiment through end faces of the sample. It penetrated into the latter without pressure, solely under gravity and capillary forces (the solution was added in small portions and the sample was always turned by 180° after this procedure). The sample was saturated with the solution up to obtaining a stable galvanic chain. Special investigations revealed that the conductivity percolation threshold is achieved when 20–25% of the sample interstices are filled with the conducting solution. This is consistent with model (theoretical) estimates of the percolation threshold based on nodes of tridimensional body-centered, face-centered, and compactly arranged hexagonal lattices [13]. In our experiments, 35–55% of the interstitial space of the sample was filled with the solution, which provided a constant excess of the conductivity percolation threshold.

We have also carried out several control experiments, in which electrodes, which provide the difference of potentials, were isolated from the sample by special placers. In these experiments, the difference of potentials was 1500 V; all other parameters were the same as in experiments with the galvanic chain (Fig. 3).

The analysis of data derived from these experiments provides grounds for the following conclusions. Flowing through samples saturated with the conducting fluid, the electric current triggers an increase in the microdestruction intensity induced by the substantial (up to 30 times) growth of AE velocity. After the electric current cut-off, the AE velocity decreases. Thus, the cyclic impact of the current results in AE modulation (Fig. 2). When the galvanic contact of electrodes with the sample is absent (when the electric chain is interrupted), although the electrostatic field provided a difference in the potential at the electrodes exists, no such modulation is observed (Fig. 3).

The analyses of variations in the incline of the repeatability plot compiled using techniques that were developed and applied for the analysis of variations in seismicity induced by the impact of powerful electric pulses [14] on the lithosphere of the Earth revealed no significant differences in these variations during time intervals with the impact of the electric current and its absence.

The electric current impact combined with an increase in the AE velocity stimulates the growth of radial deformation and axial strains in the medium controlled by the press of axial deformation (Fig. 2). No such changes in radial deformations and axial strains are observable with the impact of the electrostatic field and zero electric current (Fig. 3).

The effect of AE initiation is observed under the impact of both direct (Figs. 2a, 2b) and alternating (Fig. 2c) electric current. The analysis of variations in the difference in electric potential, impact intervals, and the concentration and volume of the NaCl solution, which determine effective electric resistivity of the sample, revealed that the AE velocity increase is mainly determined by the current power dispersed in the sample and the duration of the impact interval. The product of these two parameters corresponds to

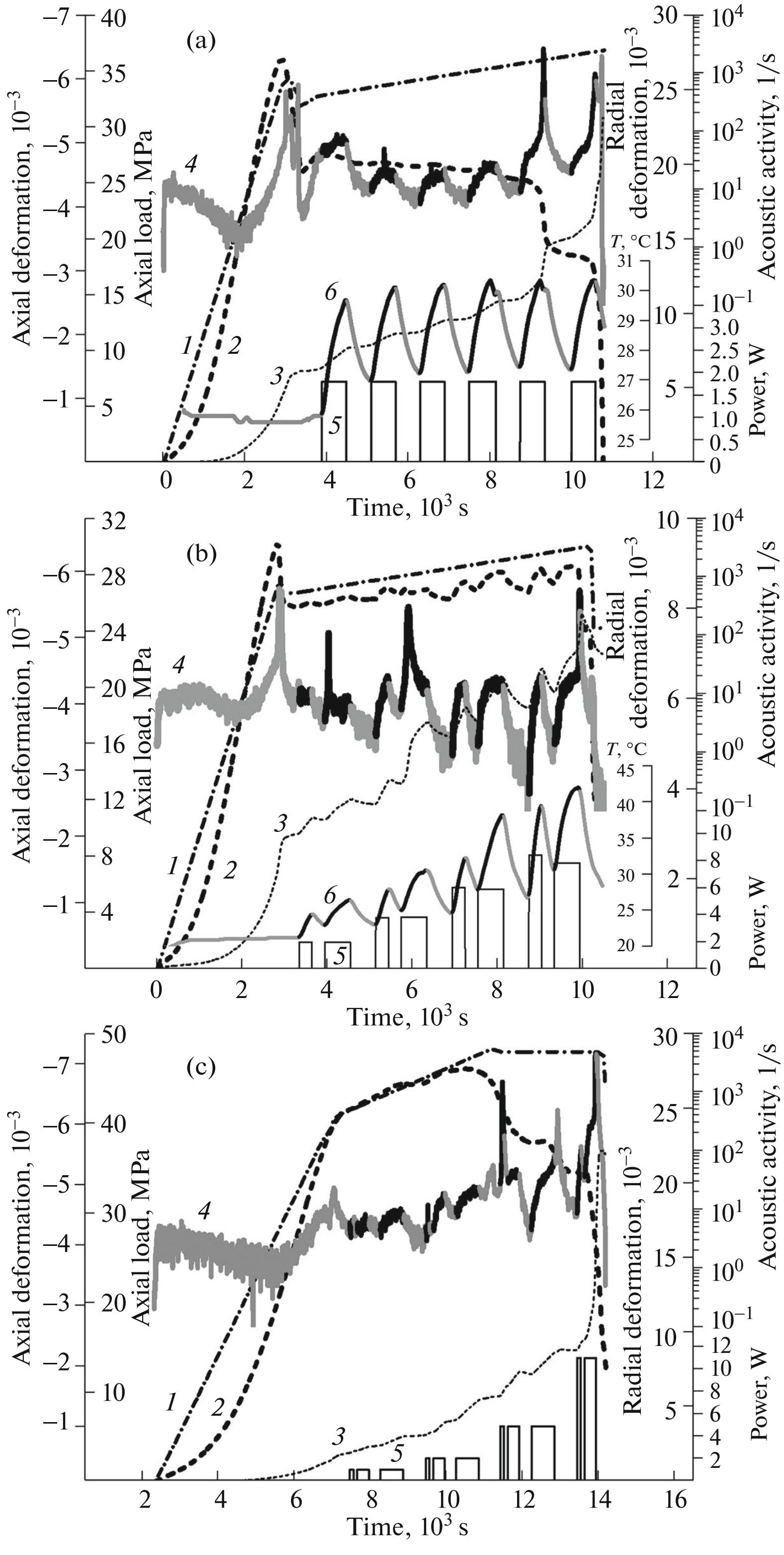

Fig. 2. Examples of variations in AE velocity under the electric current impact: (a) direct current, the same power, (b) direct current, different power levels, (c) alternating current, different power levels. Curves (here and in Fig. 3): (*1*) specified axial deformation, (*2*) axial strains, (*3*) radial deformation, (*4*) AE velocity, (5) electric power, (*6*) temperature at the cylindrical surface of the sample.

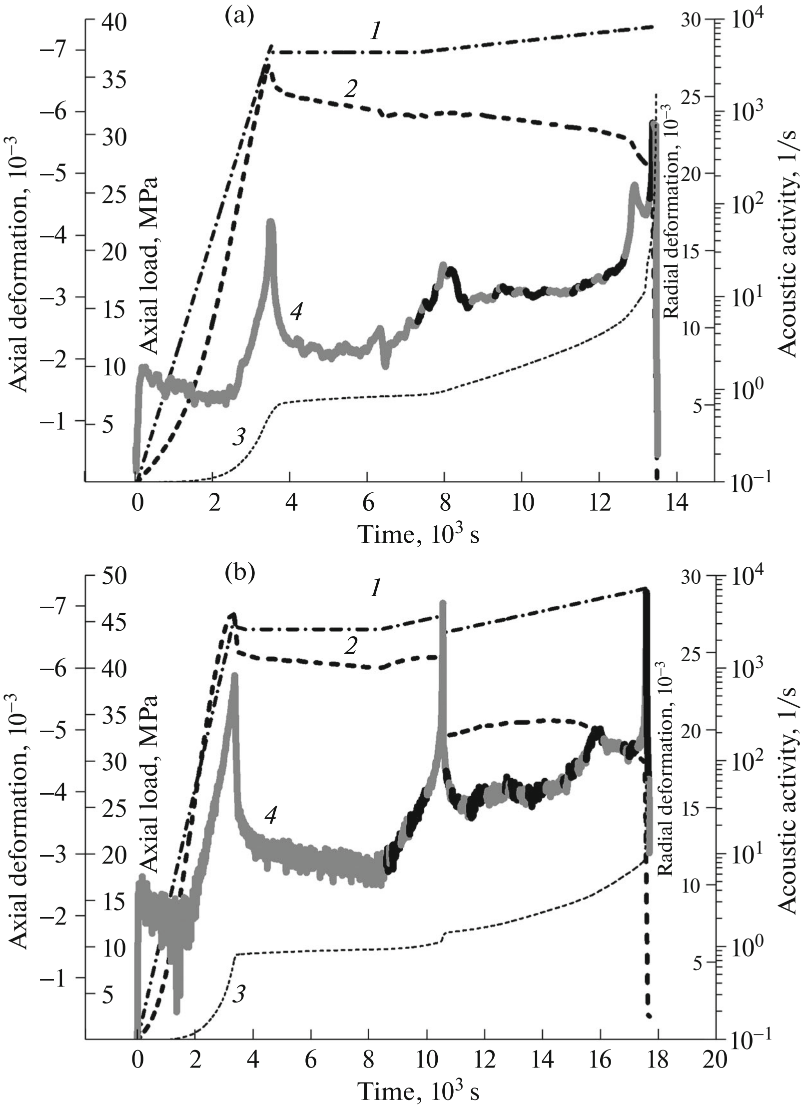

Fig. 3. Examples of variations in AE velocity under the electric current impact in the absence of galvanic contact between electrodes and the sample: (a) sample is saturated with NaCl solution, (b) dry sample. Dark areas in the curves are intervals of the impact by the difference in the electric potentials at electrodes.

the Joule heat, which is produced by the electric current. This implies that the mechanism responsible for AE initiation by the electric current is thermal in essence.

If it is accepted that the current flows in the sample owing to the fluid that fills interstices and fissures (the electric resistance of the rock is several orders of magnitude higher as compared with that of the applied NaCl solution), heating of 1 ml of the solution by the released Joule heat from dispersion of 1 W during 100 s should be as high as 23.8°C. In the experiment, the volume of the solution was 3.7 ml, the current power was 1.8 W, and the impact interval was 600 s (Fig. 2a). In such a situation, heating of the solution is estimated to be 69°C.

The heat energy of the fluid heated in interstices and fissures is spent for heating the sample, adjacent punches of the press, and sensors located on their surfaces for registering AE signals, increase of potential elastic energy of the sample owing to the growth of axial strains under axial deformation induced by the press, and, probably, destruction along microfissures. The proportion of heat energy consumed by each of these processes remains unknown. If it is assumed that all the energy is consumed by the sample, its temperature in the test medium (Fig. 2a) should increase by 14.5°C (the value of 0.8×10^3 J/(kg K) characteristic of sandstones is accepted for the heat capacity, sample mass 93 g). The experiment demonstrates that the amplitude of variations in temperature on the cylindrical surface is equal to 3°C, which corresponds approximately to 20% of Joule heat "pumped" into the sample.

When fluid in the sample is heated up to 69°C, its relative volumetric expansion is 0.03 (with the thermal expansion coefficient being 4.58×10^{-4} for temperatures of 40–60°C). Inasmuch as the sample volume is an order of magnitude larger than the fluid volume, expansion of the latter should result in sample expansion of approximately 0.003 (expansion of the sample framework during its heating by several degrees appears to be an order of magnitude lower). This value is consistent with the amplitudes of variations in radial deformation registered in the experiment, which constitute a few thousandths.

In our opinion, owing to Joule heating of the fluid contained in interstices and microfissures of the sample, its thermal expansion initiates their destruction, which is reflected in the growth of AE velocity (similar to the thermoemission effect revealed in [6] under a substantially higher thermal impact). Inasmuch as the interstitial space in rocks is filled with the fluid only partly (35–55%), some forces are required for keeping the fluid at the contact with the rock framework, which would prevent its release into the interstitial space. These forces provide the appearance of the wedging stress and could be explained by dispersion forces that appear in the space between closely located surfaces of solid bodies [15].

REFERENCES

1. M. Ya. Balbachan and I. S. Tomashevskaya, Dokl. Akad. Nauk SSSR **296** (5), 1085–1089 (1987).
2. M. A. Yaroslavskii and N. K. Kapustyan, Dokl. Akad. Nauk SSSR **315** (2), 353–354 (1990).
3. A. Zakupin, L. Bogomolov, V. Mubassarova, G. Kachesova, and B. Borovsky, in *Acoustic Emission*, Ed. by W. Sikorski (InTech, Rijeka, 2012), pp. 173–198.
4. M. S. Antsyferov, Dokl. Akad. Nauk SSSR **144** (6), 1295–1297 (1962).
5. J. Sobotka, Acta Geophys. **58** (1), 163–172 (2010).
6. V. V. Rzhevskii, V. S. Yamshchikov, and V. L. Shkuratnik, Dokl. Akad. Nauk SSSR **283** (4), 843–845 (1985).
7. D. H. Johnston and M. N. Toksoz, J. Geophys. Res. **85** (B2), 937–942 (1980).
8. Chen Yong and Chi-Yuen Wang, Geophys. Res. Lett. **7** (12), 1089–1092 (1980).
9. N. T. Tarasov, Dokl. Earth Sci. **433** (2), 1088–1091 (2010).
10. *Proc. All-Russian Seminar-Conf. on Triggered Effects in Geosystems, Moscow, June 22–24, 2010,* Ed. by V. V. Adushkin and G. G. Kocharyan (Geos, Moscow, 2010).
11. V. V. Adushkin and A. A. Spivak, *Physical Fields in Near-Surface Geophysics* (Geos, Moscow, 2014) [in Russian].
12. A. V. Patonin, A. V. Ponomarev, and V. B. Smirnov, Seism. Instrum. **50** (1), 9–19 (2014).
13. Yu. Yu. Tarasevich, *Percolation: Theory, Applications, Algorithms* (Editorial URSS, Moscow, 2002) [in Russian].
14. V. B. Smirnov and A. D. Zavyalov, Izv., Phys. Solid Earth **48** (7–8), 615–639 (2012).
15. B. V. Deryaguin, N. V. Churaev, and V. M. Muller, *Surface Forces* (Consult. Bureau, New York, 1987).

Translated by I. Basov